Volume 9 | Number 9 | 7 March 2017 | Pages 2927–3324

Nanoscale

rsc.li/nanoscale

ISSN 2040-3372

PAPER
Kyung-In Jang, Young Min Song *et al.*
Ultra-thin films with highly absorbent porous media fine-tunable for coloration and enhanced color purity

Nanoscale

PAPER

View Article Online
View Journal | View Issue

Cite this: *Nanoscale*, 2017, **9**, 2986

Published on 09 December 2016. Downloaded by PUSAN NATIONAL UNIVERSITY on 8/25/2021 5:15:32 AM.

Ultra-thin films with highly absorbent porous media fine-tunable for coloration and enhanced color purity†

Young Jin Yoo,[a] Jin Ha Lim,[b] Gil Ju Lee,[a] Kyung-In Jang*[c] and Young Min Song*[a]

Received 29th October 2016,
Accepted 9th December 2016

DOI: 10.1039/c6nr08475c

rsc.li/nanoscale

We demonstrate ultra-thin, fine-tunable optical coatings with enhanced color purity based on highly absorbent porous media on a metal substrate. We show that the color range provided by these ultra-thin film coatings can be extended by making the absorptive dielectric layer porous. Oblique angle deposition (OAD) of a thin (10–25 nm) germanium (Ge) film by e-beam evaporation onto a thick gold substrate yields controlled porosity. Reflectance spectra and color representations from both calculations and experiments verify the enhancement of resonance tunability and color purity in the nano-tailored coatings. Angle independent reflection properties, and the applicability of such porous Ge on various metal substrates, indicate the strength of these concepts.

Introduction

Thin-film optical coatings have been widely used as key elements in applications involving various optical devices.[1,2] Conventionally, optical coatings on dielectric thin-films are based on Fabry-Perot or thin-film interference. For example, anti-reflection or high-reflection is observed under conditions of constructive or destructive interference achieved by stacking layers of dielectrics with quarter wave thickness ($\lambda/4n$). Recently, highly absorptive dielectric films as optical coatings have been studied.[2–10] By combining metals with highly absorbing dielectrics, strong optical interference can be obtained with a non-trivial phase change of reflected waves. This effect allows the thickness of the coating layer to be remarkably reduced, compared to that of a conventional coating layer. With these properties, resonance behavior affecting the structural color was observed in structures composed of an ultra-thin absorbing layer (*e.g.* germanium) on a metal coated substrate.[3] The resonance in the ultra-thin film provides the colors desired or strong photon absorption, and is applicable for use in various optical components and devices including decorative solar panels,[8] coloring metals,[3,6] thin-film absorbers/emitters,[7,9] and water splitters.[10] This combination of angle-independent coloration properties and flexible applicability for electronics also offers options in engineering design that are not easily addressed with conventional thin-film optical coatings.

Although such ultra-thin film coatings are attractive, high color purity is currently constrained by inadequate materials.[5,8] Highly absorptive dielectric films, such as Ge, silicon (Si), and vanadium dioxide (VO_2), have relatively higher complex refractive indices compared to the lossless dielectric materials, in which strong resonance is prevented. The rapid color change that occurs with ultra-thin film coatings is another limitation for fine-tuning of coloration. The present work relaxes the above constraints by introducing porosity (P_r) into absorptive dielectric films. Specifically, we propose and demonstrate ultra-thin optical coatings that contain absorptive dielectric films with a 'reduced' value of the complex refractive index on a metal substrate. This combination not only generates enhanced color purity, but also simultaneously provides new design flexibility for fine-tuning of coloration. This concept is demonstrated using porous Ge layers (P_r-Ge) deposited using an oblique angle deposition (OAD) method[11–18] on an Au coated substrate. Detailed comparisons to behaviors of films formed using previous approaches illustrate the value of these techniques for enhanced performance. Optical calculation results, including reflectance spectra, chromaticity diagrams and complex reflection coefficient diagrams, also strongly support our hypothesis.

[a]School of Electrical Engineering and Computer Science, Gwangju Institute of Science and Technology, 123 Cheomdan-gwagiro, Buk-gu, Gwangju 61005, Republic of Korea. E-mail: ymsong@gist.ac.kr
[b]Department of Electrical Engineering, Pohang University of Science and Technology, 77 Cheongam-Ro, Nam-gu, Pohang 37673, Republic of Korea
[c]Department of Robotics Engineering, Daegu Gyeongbuk Institute of Science and Technology, 333 Techno Jungang-daero, Hyeonpung-myeon, Dalseong-gun, Daegu 42988, Republic of Korea. E-mail: kijang@dgist.ac.kr

† Electronic supplementary information (ESI) available. See DOI: 10.1039/c6nr08475c

 This journal is © The Royal Society of Chemistry 2017

Published on 09 December 2016. Downloaded by PUSAN NATIONAL UNIVERSITY on 8/25/2021 5:15:32 AM.

Results and discussion

Fig. 1a and b show refractive indices (n) and extinction coefficients (k) of Ge with four different P_r (*i.e.* 0%, 40%, 60% and 75%). The n and k of P_r 0% were obtained from measured data from a sample that was deposited with a 15 nm thin film of Ge at the flux angle of normal incidence using an electron beam evaporator. From these n and k values of P_r 0%, the others were obtained by effective index calculations with the other P_r values (*i.e.* 40%, 60% and 75%), based on volume averaging theory.[19] The result of the calculation proves that the higher the P_r, the lower the complex refractive index. Due to this tendency, which is scalable and gradual, optical characteristics can be controlled by managing P_r. To exploit this controllability of the optical coating, we designed a thin-film structure composed of ultra-thin Ge with P_r on a Au substrate (P_r-Ge/Au), as shown in Fig. 1c (left). At the same thickness of 20 nm, each of our proposed structures with a different P_r, had a different color, as depicted in Fig. 1c (right). For observation of this effect in terms of reflection, the calculated reflectance spectra of these structures are demonstrated in Fig. 1d. The P_r-Ge/Au has a dip in reflectance in the visible range, which is tunable, using change in the Ge thickness to alter the structural color. In our structures, the tuning of the reflective color using P_r is shown by the shift of the dip in reflectance from the long to the short wavelengths in the visible range, as P_r increases. The reason for the variability of reflectance with P_r lies in the fact that the phase change of reflection coefficients varies with P_r in the thin-film, details of which will be discussed below (see Fig. 2). Fig. 1e shows the alteration of reflectance with difference in Ge thickness (5–60 nm) for each P_r value. The contour map shows that the reflection minimum point (white dashed lines in Fig. 1e) at the higher P_r moves more slowly from short wavelengths to long wavelengths as the thickness changes.

To consider the result with P_r in terms of coloration, we conducted color representation, displayed in Fig. 1f, from the calculated reflectance (see ESI Fig. 1 and 2† for details). As the Ge thickness increases, the color at P_r 0% changes abruptly and shifts quickly to the original color of Ge. Meanwhile, that at P_r 75% changes slowly with higher color purity. For

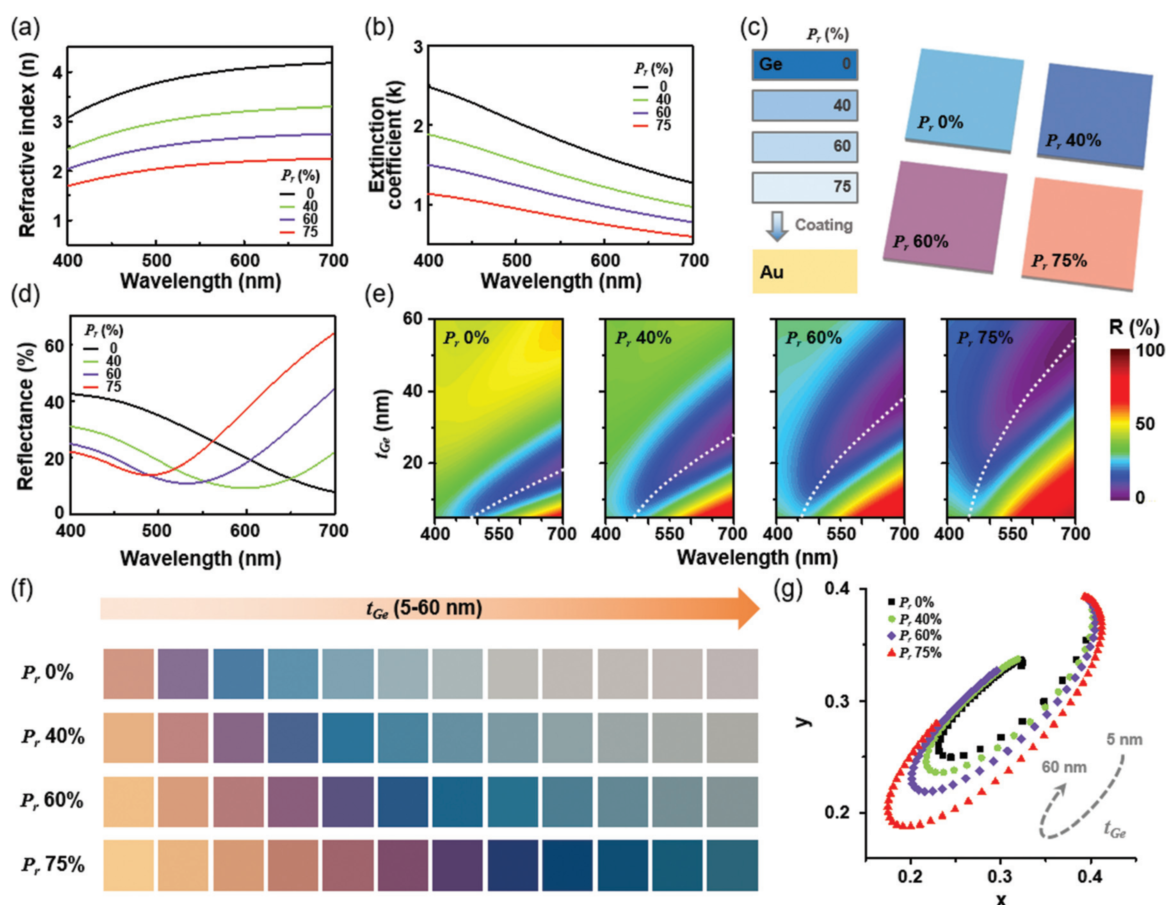

Fig. 1 (a) Calculated refractive index and (b) extinction coefficient spectra of Ge with four different porosities (P_r) (0%, 40%, 60% and 75%) as a function of wavelength. (c) Left, schematic view of proposed thin-film coatings with different P_r (*i.e.* 0%, 40%, 60% and 75%). Right, thin-film structures represented by calculated colors with different P_r (*i.e.* 0%, 40%, 60% and 75%) at the same thickness of 20 nm. (d) Calculated reflectance spectra of ultra-thin optical coatings (P_r-Ge/Au) with different P_r. (e) Contour plot of reflectance variation for P_r-Ge/Au with four different P_r as a function of Ge thickness (t_{Ge}), and of wavelength. White dashed lines in each contour plot indicate variations in the resonance dip. (f) Color representations from calculated reflectance in (e). (g) Chromaticity diagram with values obtained from (f).

Published on 09 December 2016. Downloaded by PUSAN NATIONAL UNIVERSITY on 8/25/2021 5:15:32 AM.

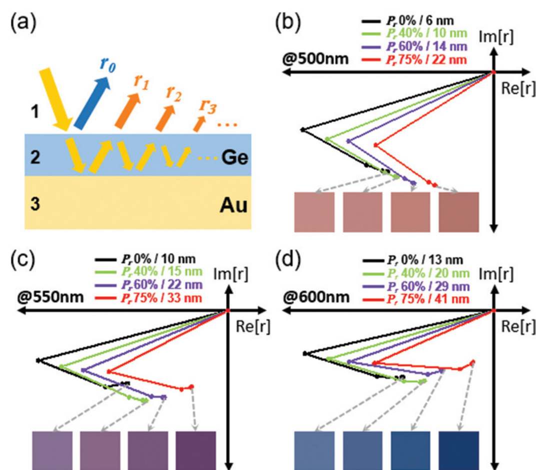

Fig. 2 (a) Schematic illustration of the reflection process in a Ge/Au thin-film structure. (b–d) Complex reflection coefficient diagram of P_r 0%, 40%, 60% and 75% at each Ge thickness enabling the minimum dip of reflectance at wavelengths of (b) 500 nm, (c) 550 nm and (d) 600 nm.

quantitative comparison of the calculated colors, chromatic diagrams at P_r 0%, 40%, 60% and 75% were plotted using coordinates on the international commission on illumination (CIE) color graph shown in Fig. 1g. Each curve, which consists of dots corresponding to increasing Ge thickness, rotates clockwise. As P_r increases, the curves cover a larger portion of the CIE color space, demonstrating the increase in color purity, which is apparent from Fig. 1f.

To analyze the effect of P_r on coloration, we considered the process of reflection from the thin-film structure, as shown in Fig. 2a. In thin-film optics, reflection can be reduced by the destructive interference of reflected waves at the surface (r_0) and at interfaces (r_1, r_2, r_3,…). Destructive interference is achievable using the quarter wavelength condition ($\lambda/4n$) in a lossless dielectric thin-film. However, this is not the case for an absorbing material because the complex refractive index causes a non-trivial phase change in the thin film. To understand the mechanism causing the minimum dip of reflectance at each of the P_r values, the total complex reflection coefficients were calculated using the following equation:[20]

$$r_{\text{total}} = \frac{r_{12} + r_{23}e^{2i\beta}}{1 + r_{12}r_{23}e^{2i\beta}}$$

where $r_{pq} = (\tilde{n}_p - \tilde{n}_q)/(\tilde{n}_p + \tilde{n}_q)$, $\tilde{n}_p = n_p + ik_p$ and $\beta = (2\pi/\lambda)\tilde{n}_2 h$. As depicted in Fig. 2b–d, using the complex plane to observe the phase change of the reflection coefficients, the results show that the end points of the phasor trajectory (with P_r 75% for all cases) are the closest to the origin (0, 0), indicating no (zero) reflection. For direct comparison, we chose the specific thickness at each P_r (0%, 40%, 60% and 75%) that gave the minimum reflection dip at the same wavelength (see ESI Fig. 3†). The colors possible for each combination of P_r value and thickness are displayed in the insets of Fig. 2b–d. Due to the low complex refractive index at P_r 75%, the surface reflection (r_0), which has significant influence on the total reflection, could be reduced. The slow phase change of the reflection coefficient with progressively thicker Ge layers, enables the sensitive control of the color.

To verify the result of the calculation previously mentioned above, we performed experiments with the OAD, allowing it to control the P_r. For the OAD of the Ge film, inclined sample holders were used. An electron beam evaporator was used to deposit the Ge film onto a substrate. A 100 nm thick layer of Au was deposited on a silicon substrate. The inclined sample holders formed oblique angles of 0°, 30°, 45° and 70° with the incident evaporated Ge flux (see ESI Fig. 4†). The OAD causes atomic shadowing and creates inclined columnar structures on the substrate, which results in increased P_r.[11] Fig. 3a shows the measured reflectance spectra from samples at each of the DAs (*i.e.* 0°, 30°, 45°, and 70° deposition angles) with different Ge thicknesses (*i.e.* 10 nm, 15 nm, 20 nm and 25 nm). As we expected, the calculation result revealed that the reflection minima shifted toward shorter wavelengths (at the same thickness) with increasing DA, and changed more slowly with different Ge thicknesses at higher DA. From these measured data, chromatic values of the fabricated samples were plotted using CIE coordinates, as shown in Fig. 3b. For comparison, the results of the calculation previously shown in Fig. 1g are also shown in Fig. 3b (dashed lines). The experimental data in the CIE color space nearly matched the calculated data, meaning that the higher the DA with a given P_r, the higher the color purity. Images of the samples corresponding to each combination of DA and Ge thickness are displayed in Fig. 3c (measurements of Ge thicknesses for all samples in ESI Fig. 5†). The real images are comparable to the color representations from the calculated values, as depicted in Fig. 1f, in terms of color change. Slight color differences between measured and calculated results derived from variations in parameters (*i.e.* P_r and t_{Ge}) during the film deposition process. It was also noted that, in the case of extreme thickness, the DA test samples that were 100 nm thick reverted to the color of Ge, as mentioned above in Fig. 1f. Scanning electron microscopy images (left images in Fig. 3c) reveal that columnar structures with different angles of inclination can be found in the P_r-Ge/Au samples fabricated at different DAs.[13,18]

To consider the angle dependency, we calculated the angle dependent reflectance of P_r 0% and 75% with particular Ge thicknesses, enabling the minimum dip to occur at wavelengths of 550 nm and 600 nm. This is depicted in the contour maps in Fig. 4a. The results show that the minimum dip remains invariant over a wide range of incident angles for all cases of both P_r 0% and 75%, and that the intensity of the dip is reduced at angles larger than 60°. In addition, the color representations of P_r 0% and 75% are plotted in Fig. 4a (left side of each contour map), which visually prove the robustness of the angle properties. We note that the high color purity of P_r 75% is also maintained with angle independence below incident angles of 60°.

Essentially, because these coatings are much thinner than the wavelengths of visible light, there is little phase difference due to the increased angle of incidence, compared with the

This journal is © The Royal Society of Chemistry 2017

Published on 09 December 2016. Downloaded by PUSAN NATIONAL UNIVERSITY on 8/25/2021 5:15:32 AM.

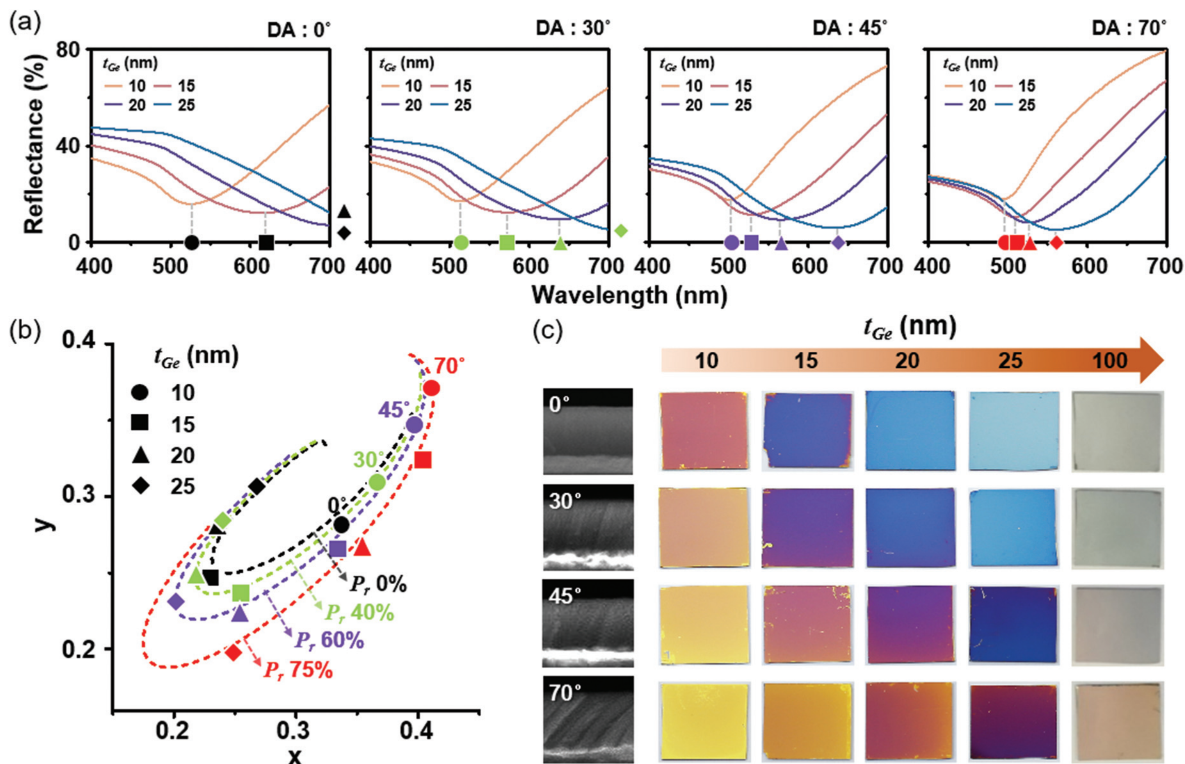

Fig. 3 (a) Measured reflectance spectra in each of deposition angles (DAs) (*i.e.*, 0°, 30°, 45° and 70°) with different Ge thicknesses (*i.e.*, 10 nm, 15 nm, 20 nm and 25 nm). (b) Chromatic values in the CIE coordinate from measured reflectance as shown in (a). Chromatic values for ultra-thin films with four different P_r (*i.e.*, 0%, 40%, 60% and 75%) are also shown by dash lines for comparison. (c) Pictures of the fabricated samples of different DAs (*i.e.*, 0°, 30°, 45° and 70°) with different Ge thicknesses (*i.e.*, 10 nm, 15 nm, 20 nm, 25 nm and 100 nm). Left, gray-scale figures show scanning microscopy images corresponding to the samples with Ge thickness of 200 nm for better showing the morphology.

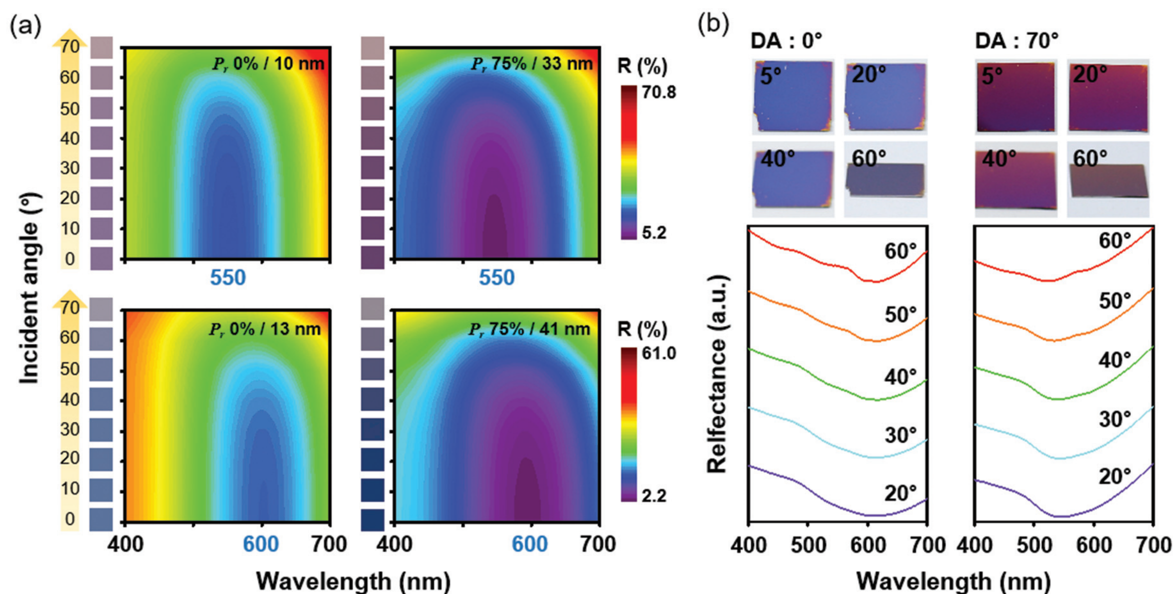

Fig. 4 (a) Contour maps of angle dependent reflectance of P_r 0% and 75% with particular Ge thicknesses having the minimum dip on reflectance at wavelengths of 550 nm and 600 nm. Colors at each incident angle for different P_r and thickness are also represented. (b) Images with different angles of view from 5° to 60° (top) and measured reflectance spectra at oblique angles from 20° to 60° (bottom) of the fabricated samples (*i.e.* t_{Ge} 15 nm at DA 0° and t_{Ge} 25 nm at DA 70°).

Published on 09 December 2016. Downloaded by PUSAN NATIONAL UNIVERSITY on 8/25/2021 5:15:32 AM.

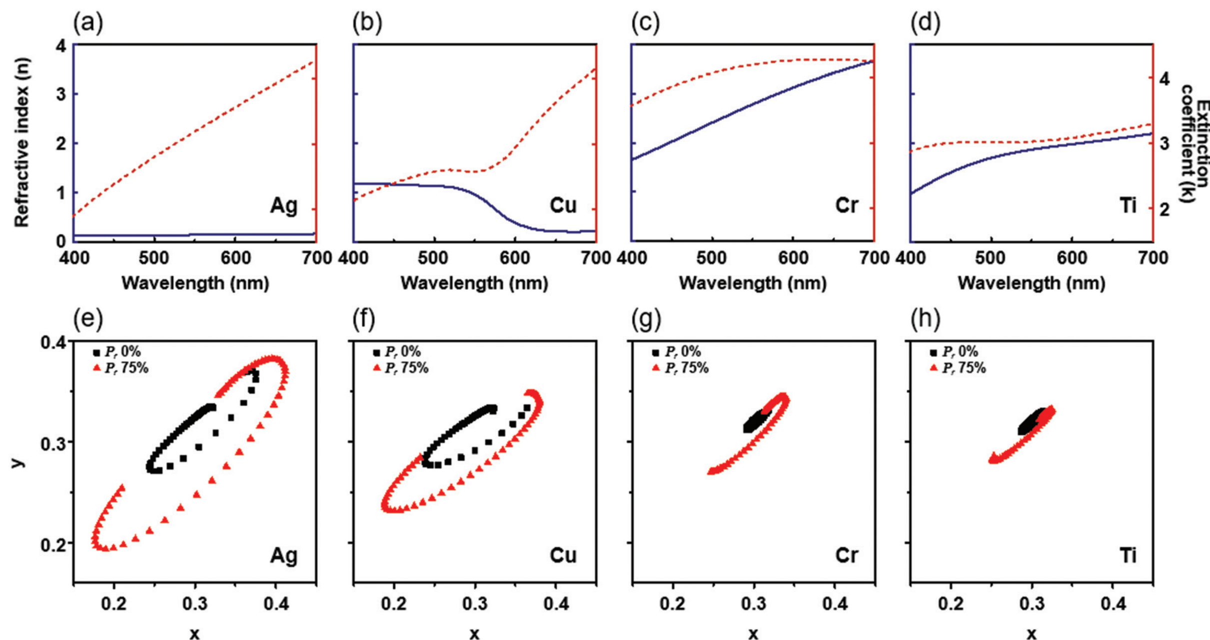

Fig. 5 (a–d) Refractive indices and extinction coefficients of (a) Ag, (b) Cu, (c) Cr and (d) Ti. (e–h) Calculated chromatic values of P_r 0% and 75% with (e) Ag, (f) Cu, (g) Cr and (h) Ti in CIE coordinates.

case of normal incidence. Although the Ge thickness at P_r 75% is thicker than that of P_r 0% at the same dip in the reflectance, the phase difference of P_r 75% with the angle of incidence is similar to that of P_r 0% due to the lower complex effective index of P_r 75%.

For the validity of the previous calculation, images of DA 0° and 70° samples were taken at viewing angles of 5°, 20°, 40° and 60°. The reflectance spectra of DA 0° and 70° were measured at angles of incidence ranging from 20° to 60°, as shown in Fig. 4b (shown for all samples in ESI Fig. 6†). There is no color change for both DA 0° and 70° up to the angle of 60° (Fig. 4b top). The position of the minimum dip for all cases of DA 0° and 70° is maintained within the shape of the curve (Fig. 4b bottom).

For universality, we conducted additional calculations for several cases with different metals (*i.e.* silver, copper, chromium, and titanium), as shown in Fig. 5. Conceptually, an ideal perfect metal, corresponding to complete reflection with a phase shift of π, is not suitable for ultrathin coatings ($t \ll \lambda/4n$). To obtain strong resonance with an ultra-thin film, a highly reflective metal is needed, among those metals having a non-trivial phase change. Ag is a highly reflective metal with low n and high k (Fig. 5a). Cu has higher reflectivity, with decreasing n and increasing k at longer visible wavelengths (Fig. 5b). Cr and Ti have relatively low reflectivity with high n (Fig. 5c and d). As expected, the result in the case of Ag shows that the chromatic values of P_r 0% cover a reasonable portion in the CIE color space and those curves with P_r 75% cover an enhanced large portion (Fig. 5e). Interestingly, the chromatic curves typical of Cu, cover a one-sided area in both cases of P_r 0 and 75% (Fig. 5f). Although P_r 0% of Cr and Ti show small areas of coverage in the color space, at P_r 75% their coverage area slightly increases. From the results mentioned above, it is noted that applying P_r to Ge shows expansion of the color area in all the cases we have considered.

Conclusions

In summary, we have demonstrated a structure consisting of thin-Ge films with different P_r values on Au. Our proposed structures were investigated using optical calculations and sample fabrication using OAD. The calculated reflectance results reveal that the optical resonance can be tuned by managing P_r values for a structure of the same thickness. From considerations in terms of color and reflection coefficients, the results demonstrate that the most sensitive controllability of the resonance dip shift and high color purity was obtained with P_r 75%. The results from fabricated samples were comparable to the calculated results, including those for reflectance and color representation. In particular, the highest performance was achieved at DA 70° (similar to that of P_r 75%). The results prove the suitability of OAD for the control of P_r in thin-film layers. In thin-film optical coatings, P_r controllable by the OAD could be an additional parameter for tuning the optical resonance. Furthermore, other materials could be used with our design with P_r to obtain better performance. Hence, we expect our proposed concept could be widely used as an effective method to enhance the optical characteristics needed in applications including colorizing metals, optical filters, and thin-film absorbers.

 This journal is © The Royal Society of Chemistry 2017

Published on 09 December 2016. Downloaded by PUSAN NATIONAL UNIVERSITY on 8/25/2021 5:15:32 AM.

Methods

Sample preparation

Prior to film deposition, semi-insulated, single-side polished silicon (100) wafers were soaked in buffered oxide etchant (BOE) for 3 min to remove the native oxide; then cleaned with acetone followed by deionized water. Both Au and Ge films were deposited using electron beam evaporation (KVE-E2000, Korea Vacuum Tech Ltd, Korea). The Au film was deposited on a Si substrate at a rate of ~2 Å s^{-1} and a pressure of ~10^{-6} torr. The thickness of Au was 100 nm, and this was judged sufficient optical thickness (see ESI Fig. 7†). Ge thin-films were deposited on the Au film using (customized) inclined sample holders at different angles (*i.e.*, 0°, 30°, 45° and 70°) at a rate of ~1 Å s^{-1} and a pressure of ~10^{-6} torr.

Characterization

The reflectance of the fabricated samples was measured using a UV-Vis-NIR spectrophotometer (Cary 500, Varian, USA) at a normal angle of incidence with a tungsten-halogen lamp source. The angle dependent reflection spectra were obtained using a variable-angle specular reflectance accessory (VARSA). The optical constants of the Ge films were measured using spectroscopic ellipsometry (UVISEL ER Benchtop AGAS, Horiba Korea Ltd). The P_r-Ge/Au samples with Ge thickness of 100 nm were characterized by field emission SEM (S-4700, Hitachi, Japan) with an operating voltage of 10 kV.

Simulations

The RCWA method was used to calculate the reflectance of the proposed structures using commercial software (Diffract MOD, RSoft Design Group, USA).[20] In the RCWA calculation, a second diffraction order and grid size of 0.2 nm were used to calculate the diffraction efficiency, which is enough to stabilize the results numerically. The non-polarized light reflectance was calculated by averaging the reflectance for p- and s-polarization. Material dispersions and extinction coefficients were considered for obtaining exact outputs. The commercial MATLAB (Mathworks, Inc.) software was also used to calculate both the complex reflection coefficient in the thin-film structure, and the chromatic information from the reflectance.[21–24]

Acknowledgements

This work was supported by a National Research Foundation of Korea grant (NRF no. 2015R1A5A7036513), funded by the Korean Government (MSIP).

References

1 H. A. Macleod, *Thin-film optical filters*, Institute of Physics Publishing, 3rd edn, 2001.
2 P. W. Baumeister, *Optical Coating Technology*, SPIE Press, Bellingham, Washington, 2004.
3 M. A. Kats, R. Blanchard, P. Genevet and F. Capasso, *Nat. Mater.*, 2012, **12**, 20–24.
4 M. A. Kats, D. Sharma, J. Lin, P. Genevet, R. Blanchard, Z. Yang, M. M. Qazilbash, D. N. Basov, S. Ramanathan and F. Capasso, *Appl. Phys. Lett.*, 2012, **101**, 221101.
5 M. A. Kats, S. J. Byrnes, R. Blanchard, M. Kolle, P. Genevet, J. Aizenberg and F. Capasso, *Appl. Phys. Lett.*, 2013, **103**, 101104.
6 K. T. Lee, S. Seo, J. Y. Lee and L. J. Guo, *Adv. Mater.*, 2014, **26**, 6324–6328.
7 H. Song, L. Guo, Z. Liu, K. Liu, X. Zeng, D. Ji, N. Zhang, H. Hu, S. Jiang and Q. Gan, *Adv. Mater.*, 2014, **26**, 2737–2743.
8 X. L. Zhang, J. F. Song, X. B. Li, J. Feng and H. B. Sun, *Appl. Phys. Lett.*, 2013, **102**, 103901.
9 W. Streyer, S. Law, G. Rooney, T. Jacobs and D. Wasserman, *Opt. Express*, 2013, **21**, 9113–9122.
10 H. Doten, O. Kfir, E. Sharlin, O. Blank, M. Gross, I. Dumchin, G. Ankonina and A. Rothschild, *Nat. Mater.*, 2013, **12**, 158–164.
11 K. Robbie, J. C. Sit and M. J. Brett, *J. Vac. Sci., Technol. B*, 1998, **16**, 1115–1122.
12 M. M. Hawkeye and M. J. Brett, *J. Vac. Sci. Technol. A*, 2007, **25**, 1317–1335.
13 S. J. Jang, Y. M. Song, J. S. Yu, C. I. Yeo and Y. T. Lee, *Opt. Lett.*, 2011, **36**, 253–255.
14 S. J. Jang, Y. M. Song, C. I. Yeo, C. Y. Park and Y. T. Lee, *Opt. Mater. Express*, 2011, **1**, 451–457.
15 K. D. Harris, A. C. V. Popta, J. C. Sit, D. J. Broer and M. J. Brett, *Adv. Funct. Mater.*, 2008, **18**, 2147–2153.
16 Y. Zhong, Y. C. Shin, C. M. Kim, B. G. Lee, E. H. Kim, Y. J. Park, K. M. A. Sobahan, C. K. Hwangbo, Y. P. Lee and T. G. Kim, *J. Mater. Res.*, 2008, **23**, 2500–2505.
17 G. K. Kiema, M. J. Colgan and M. J. Brett, *Sol. Energy Mater. Sol. Cells*, 2005, **85**, 321–331.
18 J. K. Kim, S. Chhajed, M. F. Schubert, E. F. Schubert, A. J. Fischer, M. H. Crawford, J. Cho, H. Kim and C. Sone, *Adv. Mater.*, 2008, **20**, 801–804.
19 A. Garahan, L. Pilon, J. Yin and I. Saxena, *J. Appl. Phys.*, 2007, **101**, 014320.
20 M. G. Moharam, *Proc. SPIE*, 1988, **883**, 8–11.
21 M. Born and E. Wolf, *Principles of Optics: Electromagnetic Theory of Propagation, Interference and Diffraction of Light*, Cambridge Univ. Press, 7th edn, 1999.
22 T. Smith and J. Guild, *Trans. Opt. Soc.*, 1931, **33**, 73.
23 R. L. Olmon, B. Slovick, T. W. Johnson, D. Shelton, S. H. Oh, G. D. Boreman and M. B. Raschke, *Phys. Rev. B: Condens. Matter*, 2012, **86**, 235147.
24 N. Ohta and A. R. Robertson, CIE Standard Colorimetric System, in *Colorimetry: Fundamentals and Applications*, John Wiley & Sons, Ltd, Chichester, UK, 2005.